electronic band. In this respect, phosphides have advantages over nitrides, such as isostructural Li_7MnN_4 (*19*), and the layered compounds $Li_{2.6-x}Co_{0.4}N$ (*6*, *7*) and $Li_{2.7}Fe_{0.3}N$ (*20*), proposed as negative electrodes. Differences in the strength of the M-pnictogen (P_N) bond and the relative contribution of the P_N–P_N bond result in a paucity of transition metal–poor binary nitrides; for example, MnN_4, analogous to MnP_4, does not exist. Because no binarynitrides are known that can reversibly uptake Li^+/e^-, the ternary nitrides must first be "charged" by electrochemical oxidation of Li from the structure, a drawback of these materials that also results in collapse to an amorphous structure. More importantly, the negative electrode in a cell should act as a reservoir for Li, as MnP_4 does, not a source.

In conclusion, the behavior of the phosphides represents a departure from that exhibited by ionic negative electrode materials, such as oxides (where the high energy of the metal-localized bands drives the reduction to the metallic state on Li uptake); nitrides; and intermetallic negative-electrode materials, where Li uptake relies on the formation of alloys Li_xM (M = Sb or Sn). Furthermore, facile covalent-bond rearrangement and atom migration that lead to electrochemical "recrystallization" are a signature of phosphides. New opportunities afforded by these materials will be explored in our forthcoming work (*21*), including iron and cobalt phosphides, where control of microstructure will be investigated as a route to facilitate structural conversion.

References and Notes

1. M. S. Whittingham, A. J. Jacobson, *Intercalation Chemistry* (Academic Press, New York, 1982).
2. M. Winter, J. O. Besenhard, M. E. Spahr, P. Novak, *Adv. Mater.* **10**, 725 (1998).
3. T. Ohzuku, A. Ueda, N. Yamomoto, *J. Electrochem. Soc.* **142**, 1431 (1995).
4. B. A. Boukamp, G. C. Lesh, R. A. Huggins, *J. Electrochem. Soc.* **128**, 725 (1981).
5. I. A. Courtney, J. R. Dahn, *J. Electrochem. Soc.* **144**, 2045 (1997).
6. T. Shodai, Y. Sakurai, T. Suzuki, *Solid State Ionics* **122**, 85 (1999).
7. Y. Takeda *et al.*, *Solid State Ionics* **130**, 61 (2000).
8. P. Poizot, S. Laruelle, S. Grugeon, L. Dupont, J.-M. Tarascon, *Nature* **407**, 499 (2000).
9. M. N. Obrovac, R. A. Dunlap, R. J. Sanderson, J. R. Dahn, *J. Electrochem. Soc.* **148**, A576 (2001).
10. K. D. Kepler, J. T. Vaughey, M. M. Thackeray, *Electrochem. Solid-State Lett.* **2**, 307 (1999).
11. G. X. Wang, L. Sun, D. H. Bradhurst, S. X. Dou, H. K. Liu, *J. Alloys Compounds* **299**, L12 (2000).
12. We use the term "topotactic" to imply a definite relation between crystallographic directions in the reactant and the product; the precise transformation mechanism is currently under investigation.
13. W. Jeitscko, P. C. Donahue, *Acta Crystallogr. B* **31**, 574 (1975).
14. Forty-three reflections observed out of a total of 43 (relative intensity >1) listed in the Joint Committee on Powder Diffraction Studies #30-0822; refined lattice parameters (LeBail method): a = 10.513 Å; b = 5.096 Å; c = 21.81 Å; β = 94.68°.
15. T. Kerr, J. Gaubicher, L. F. Nazar, *Electrochem. Solid-State Lett.* **3**, 460 (2000).
16. The contribution from lithium insertion into the carbon used as the additive in the electrode preparation is excluded from this value.
17. W. Weppner, R. A. Huggins, *J. Electrochem. Soc.* **124**, 1569 (1977).
18. Cleavage of anion-anion bonds along with reduction of the cation has been observed in the insertion of Li into TiS_3 [e.g., D. W. Murphy, F. A. Trumbore, *J. Electrochem. Soc.* **123**, 960 (1976)].
19. S. Suzuki, T. Shodai, *Solid State Ionics* **116**, 1 (1999).
20. J. L. C. Rowsell, V. Pralong, L. F. Nazar, *J. Am. Chem. Soc.* **123**, 8598 (2001).
21. V. Pralong, D. C. S. Souza, K. T. Leoung, L. F. Nazar, *Electrochem. Commun.* **4**, 516 (2002).

22. L.F.N. gratefully acknowledges the Natural Sciences and Engineering Research Council of Canada for funding this work, D.C.S. thanks CAPES/Brazil for financial support.

20 February 2002; accepted 19 April 2002

Co-Seismic Strike-Slip and Rupture Length Produced by the 2001 M_s 8.1 Central Kunlun Earthquake

Aiming Lin,[1]* Bihong Fu,[1] Jianming Guo,[2] Qingli Zeng,[3] Guangming Dang,[4] Wengui He,[5] Yue Zhao[3]

Field investigations show that the surface wave magnitude (M_s) 8.1 Central Kunlun earthquake (Tibetan plateau) of 14 November 2001 produced a nearly 400-kilometer-long surface rupture zone, with as much as 16.3 meters of left-lateral strike-slip along the active Kunlun fault in northern Tibet. The rupture length and maximum displacement are the largest among the co-seismic surface rupture zones reported on so far. The strike-slip motion and the large rupture length generated by the earthquake indicate that the Kunlun fault partitions its deformation into an eastward extrusion of Tibet to accommodate the continuing penetration of the Indian plate into the Eurasian plate.

Strike-slip faults often play an important role in horizontal extrusions of the lithosphere away from continental collision zones (*1*). The Tibetan plateau is a unique natural laboratory for studying collisional strike-slip faulting processes. There numerous tectonic blocks, some hundreds of kilometers wide, are moving eastward and southeastward along some major strike-slip faults to accommodate the ongoing northward penetration of the Indian plate into the Eurasian plate (*2*–*5*). The eastward extrusion of Tibet has generated 11 great earthquakes (with magnitudes between 7.5 and 8.7) in the past 300 years along the major strike-slip faults that bound the north side of Tibet (*6*). The 1200-km-long Kunlun fault striking E-W to WNW-ESE is one of the major collisional strike-slip faults in the Tibetan plateau (Fig. 1).

The M_s 8.1 Central Kunlun earthquake occurred on 14 November 2001 in the Kunlun mountain area (Fig. 1) (*7*). There were no reports of casualties or major damage, because the earthquake was centered in a remote area that is relatively flat, with elevation ranging between 4500 and 6860 m along the Kunlun fault. The motion on the fault due to the earthquake could not be determined from the seismic data (*8*–*11*) [Fig. 1 and table S1 (*12*)]. To determine the motion of the fault at the surface, the co-seismic displacement, and the rupture length, our survey group went to the epicentral area 5 days after the event.

The field investigations show that a nearly 400-km-long co-seismic surface rupture zone, called the Kunlun rupture zone hereafter, occurred mostly along the western (Kusai Lake) segment of the Kunlun fault (Fig. 1). The Kunlun fault cuts the south-sloping alluvial fans and bajada in the study area, which is recognized as a straight lineament trending E-W to WNW-ESE in the satellite images that were used for field mapping (Fig. 1). The surface ruptures were concentrated in a zone with a width ranging from 3 to 550 m, with an average width of 5 to 50 m. The zone is composed of distinct shear faults, extensional cracks, and mole tracks [Fig. 2 and figs. S1 and S2 (*12*)], mostly along the fault lineament shown in the satellite image (Fig. 1). The distinct shear fault planes were observed at sites 3 to 8, which strike N75°W to E-W, dip 75° to 90°N, and are parallel to the general trend of the surface rupture zone [Fig. 2B and fig. S1C (*12*)]. Horizontal slickenside striations were observed on the shear fault planes, which are marked by parallel lineations with some grooves and steps in the frozen allu-

[1]Institute of Geosciences, Faculty of Science, Shizuoka University, 836 Ohya, Shizuoka 422–8529, Japan. [2]Lanzhou Institute of Geology, Chinese Academy of Sciences, Lanzhou 730000, China. [3]Institute of Geomechanics, Chinese Academy of Geological Sciences, Beijing 100081, China. [4]Seismological Bureau of Qinghai Province, Xining, China. [5]Seismological Institute of Lanzhou, Lanzhou 730000, China.

*To whom correspondence should be addressed. E-mail: slin@ipc.shizuoka.ac.jp

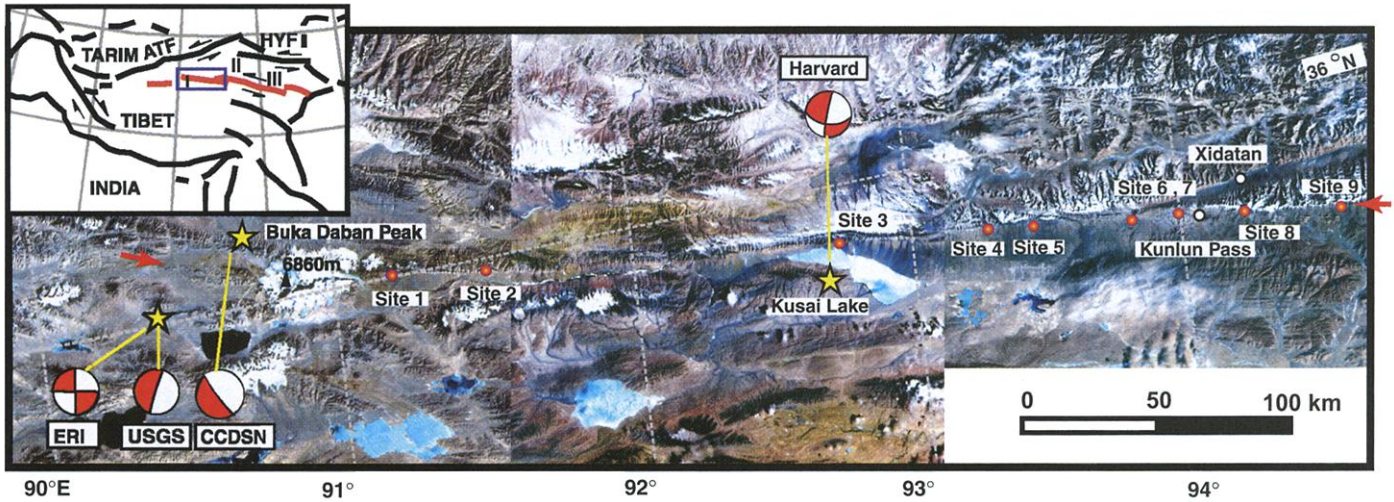

Fig. 1. Satellite image showing the Kunlun fault (indicated by red arrows) in the study area. The locations of epicenters (indicated by stars) and focal mechanisms of the 2001 M_s 8.1 Central Kunlun earthquake were determined by CCDSN (*8*), ERI (*9*), Harvard (*10*), and USGS (*11*). GRI, Geophysical Research Institute, China Seismological Bureau (*8*). I, Kusai Lake segment; II, Xidatan segment; III, Tuosho Lake segment of the Kunlun fault in the index map; ATF, Altyn Tagh fault; HYF, Haiyuan fault. Small arrows indicate the movement sense of the fault. Sites 1 to 9 (indicated by red solid circles) where the displacements were measured are located on the Kunlun fault.

vial deposits of clay, fine-grained sand, and gravel (Fig. 2B). The extensional cracks commonly show a right-stepping echelon pattern that indicates a left-lateral sense of shear, and they were widespread along the surface rupture zone (Fig. 2C). The mole tracks, 30 cm to 3 m high, were formed in the area between two adjacent shear faults [fig. S1A (*12*)]. These coseismic deformation characteristics of surface markers and slickenside striations on the fault planes reveal that the earthquake had a left-lateral strike-slip motion at the surface.

The displacements were measured along the rupture zone by means of offsets of linear surface markers such as moraines, roads, stream channels, gullies, and terraces, which were generally perpendicular to the surface rupture zone [Fig. 2A, figs. S1 and S2, and table S2 (*12*)]. The displacements were measured at seven sites in the eastern segment of the rupture zone (from 92° to 95°E). However, the western segment of the rupture zone located in the region (from 90° to 92°E), crowned by high mountains (with a maximum elevation of 6860 m at the Buka Daban Peak), glaciers, and marshes, was too difficult to access. Therefore, displacements were measured at only two sites (sites 1 and 2 in Fig. 1) in the western segment of the rupture zone. The surface rupture zone was recognized in the westernmost location ~15 km west from site 1, but the western end of the rupture zone was not investigated in this study. The maximum displacement of 16.3 m was measured along three distinct shear faults and six narrow extensional crack zones, which form a rupture zone of 550 m on a stream channel along the eastern segment at site 4 [Fig. 3 and figs. S1F and S3 (*12*)]. At site 5, a present-day moraine that consists mainly of ice boulders was sinistrally offset 13.5 m along the rupture zone, which was ~30 m wide (Fig. 2A). These deformational characteristics of the surface features indicate that the large displacements were produced by the event. The displacements observed at sites 1 and 9 and the ruptures recognized in the westernmost location indicate that the rupture length is at least ~400 km (Figs. 1 and 3). Both the rupture length and the maximum displacement observed from this earthquake are the

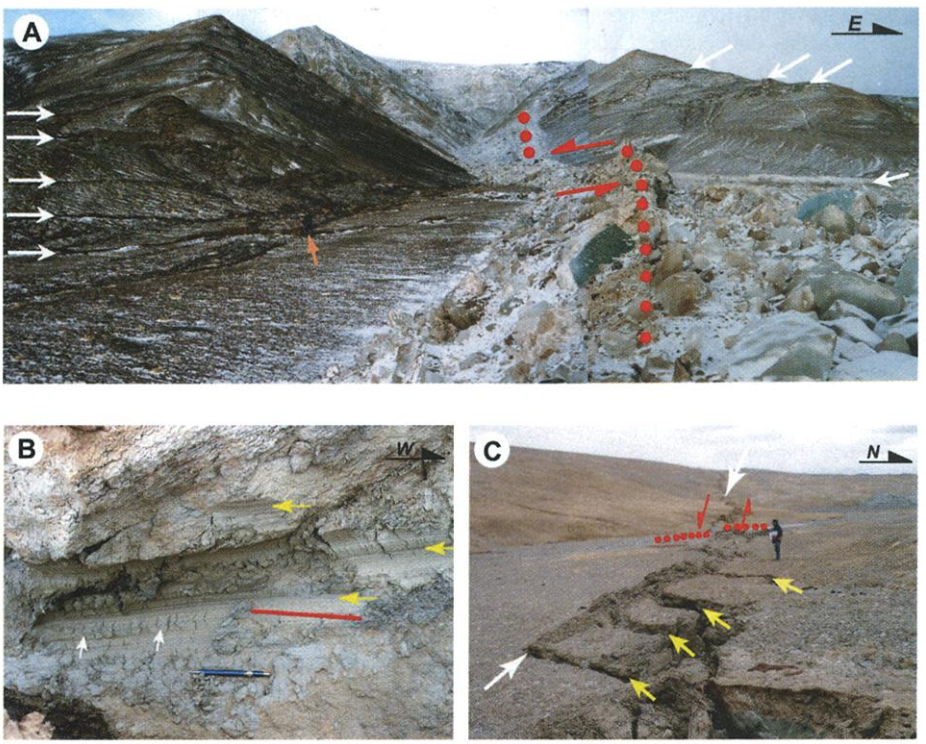

Fig. 2. Typical outcrops of the Kunlun rupture zone. (**A**) Left-lateral strike-slip of the present-day moraine (indicated by red solid circles) along the rupture zone (site 5). The rupture zone is composed of five major shear faults (indicated by white arrows) and many cracks. The present-day moraine is sinistrally offset about 13.5 m along the surface rupture zone, which is ~30 m wide. The scale is shown by the man (indicated by small yellow arrow). The view is toward the north. (**B**) Slickenside striations (indicated by yellow arrows) and steps (indicated by white arrows) developed during the earthquake on the shear fault plane (site 7). The striations are almost parallel to the horizontally oriented red line and the pen. Pen scale, 15 cm. The view is toward the south. (**C**) Right-stepping echelon extensional cracks (indicated by yellow arrows, site 7). The stream channel (indicated by red solid circles) is sinistrally offset 6.8 m along the rupture zone (indicated by white arrows). The view is toward the west.

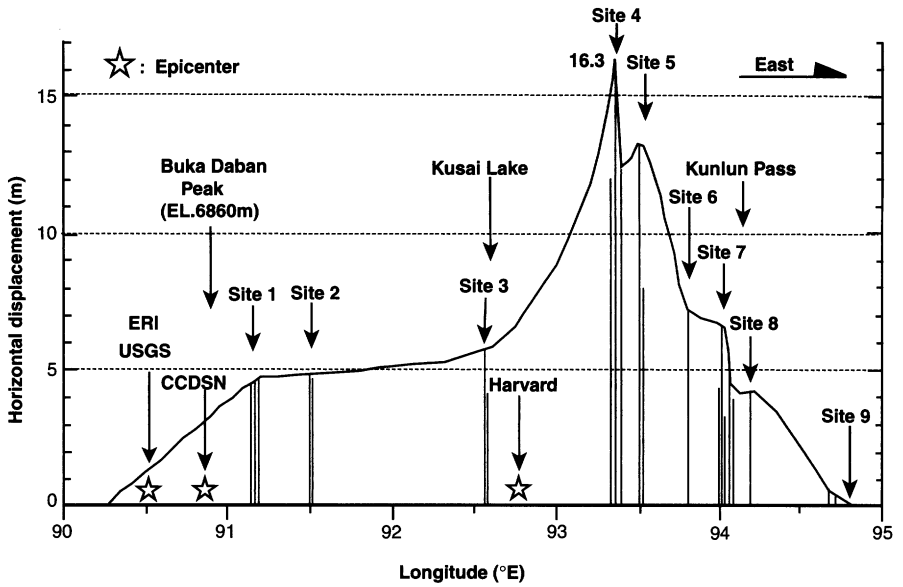

Fig. 3. Details of left-lateral strike-slip measured along the Kunlun rupture zone. All locations of sites 1 to 9 and of epicenters are shown in Fig. 1. Detailed data on the displacements are shown in table S2 (*12*).

largest among the co-seismic surface rupture zones ever reported (*1*). The large displacement and rupture length are of great importance as key parameters in estimating maximum earthquakes and earthquake moments and assessing individual seismogenic structures for the Kunlun fault and other strike-slip faults in the Tibetan plateau.

The focal mechanism solutions for the Central Kunlun earthquake given by the Earthquake Research Institute (ERI) of the University of Tokyo (*9*) and by Harvard (*10*) show that the two nodal faults strike nearly E-W and N-S, which is consistent with what we observed in the field. However, the China Center of Digital Seismic Network (CCDSN) (*8*) and the U.S. Geological Survey (USGS) (*11*) gave different nodal faults for the event [table S1 (*12*)]. Other parameters obtained from the focal mechanism solutions, such as the epicenter and rupture length, are also different from the field observation [table S1 (*12*)]. The focal mechanism solution of ERI (*9*) shows that the subsurface rupture length was ~200 km, with an average and maximum strike-slip of 3.6 m and 6 m, respectively. It is difficult to determine the attitude of the fault, the rupture length, the displacement, and the epicenter of the Central Kunlun earthquake by using seismic data alone. Field investigation is necessary for reconfirming the focal mechanism solutions obtained from the seismic data and for understanding the earthquake faulting process.

Based on satellite images, cosmogenic surface dating (*13*, *14*), and trenching surveys (*15*), the Kunlun fault has been inferred to be active and to have left-lateral motion on a strike-slip fault. The Kunlun fault absorbs a substantial amount of the present-day convergence between the Indian plate and the Eurasian plate by allowing the Tibetan plateau to move northward (*5*, *16*). Two historic large earthquakes occurred along the fault: (i) the 1937 M 7.5 Tuosho Lake earthquake, which ruptured the Tuosho Lake segment (Fig. 1) of the Kunlun fault and produced a 300-km-long surface rupture zone between 96°E and 99°E, with a maximum left-lateral strike-slip of 6 m (*17*); and (ii) the 1997 M_w 7.6 Manyi earthquake at the Quaternary fault, which produced a 170-km-long surface rupture zone between 86°E and 88°E, with a maximum left-lateral strike-slip of 7 m (*18*). The Quaternary fault is considered to be a branch fault of the Kunlun fault system. Although there is no historic earthquake recorded in the Xidatan segment between the Kusai Lake segment and the Tuosho Lake segment (Fig. 1) along the Kunlun fault, it has been inferred that great earthquakes (M ~8) recurred in this segment with characteristic left-lateral strike-slip of 9 to 12 m every 800 to 1000 years, based on the cosmogenic surface dating of offset alluvial terraces (*13*, *14*) and trenching surveys (*15*). The left-lateral strike-slip and rupture length derived from paleoseismic studies of the large earthquakes of M 7.5 to 8.0 are compatible with those derived in this study. With the assumption of a recurrence interval of 800 to 1000 years and the maximum strike-slip of 16.3 m produced by the Central Kunlun earthquake, a maximum slip rate of 16 to 20 mm/year is inferred for this segment of the Kunlun fault. This maximum left-lateral strike-slip rate is similar to the Pleistocene average rates for the other segments: 10 to 20 mm/year for the Kusai Lake segment (*19*) and ~12 ± 2.0 mm/year for the Xidatan and Tuosho segments (*13*, *14*). It was estimated that the left-lateral strike-slip of the Kunlun fault accounts for 30 to 50% of the eastward component of motion of Tibet relative to the Gobi desert (*13*, *14*, *20*). Global Positioning System results show that north Tibet moves east-northeastward at a rate of ~8 mm/year (*21*, *22*), and south central Tibet moves at ~20 to 22 mm/year to the east-northeast (*22*, *23*) with respect to Eurasia. The large left-lateral strike-slips produced by the Central Kunlun earthquake and the estimated recurrence interval of 800 to 1000 years (*13*, *14*) imply that the differential motion of 12 to 14 mm/year between north Tibet and south central Tibet (*22*) is accommodated by the Kunlun fault as seismic slip. Our fieldwork on the Kunlun fault documents and confirms that large-scale strike-slip motion along a major east-west–trending fault can accommodate the continuing penetration of India into Asia by the eastward extrusion of Tibet (*4*, *5*, *14*, *16*, *20*).

References and Notes

1. R. S. Yeats, K. Sieh, C. R. Allen, *The Geology of Earthquake* (Oxford Univ. Press, Oxford, 1997).
2. P. Molnar, P. Tapponnier, *Science* **189**, 419 (1975).
3. ———, *J. Geophys. Res.* **83**, 5361 (1978).
4. J. P. Avouac, P. Tapponnier, *Geophys. Res. Lett.* **20**, 895 (1993).
5. B. Meyer *et al.*, *Geophys. J. Int.* **135**, 1 (1998).
6. G. Gu, T. Li, A. Shen, *Catalogue of Chinese Earthquakes (1831 BC-1969 AD)* (Science Press, Beijing, 1989).
7. China Seismological Bureau, "2001 Qinghai M_s 8.1 earthquake" (http://210.72.96.1/focus-hot/qingcmt-comp.htm) (last accessed 6 June 2002).
8. CCDSN, "Moment tensor solution of Qinghai-Xinjiang earthquake" (http://210.72.96.1/focus-hot/qingcmtcomp.htm) (last accessed 6 June 2002).
9. M. Kikuchi, Y. Yamanaka, ERI, University of Tokyo, "Earthquake note no. 111" (http://wwweic.eri.u-tokyo.ac.jp/topics/200111140926/index-j.html) (last accessed 23 January 2002).
10. Harvard University, "Centroid, moment tensor solution" (Harvard Event-File Name M111401A, http://wwweic.eri.u-tokyo.ac.jp/~cmt/HARVARD/CMT/November14200192710) (last accessed 6 June 2002).
11. USGS, "Rapid moment tensor solution of Southern Xinjiang earthquake, China" (http://wwweic.eri.u-tokyo.ac.jp/~cmt/USGS/CMT0111140926) (last accessed 6 June 2002).
12. Supporting online material is available on *Science* Online.
13. J. Van der Woerd *et al.*, *Geology* **26**, 695 (1998).
14. J. Van der Woerd *et al.*, *Geophys. Res. Lett.* **27**, 2353 (2000).
15. G. Zhao, *Earthquake Res. China* **12**, 107 (1996).
16. P. Molnar *et al.*, *Geology* **15**, 249 (1987).
17. Y. Jia *et al.*, in *Research on Earthquake Faults in China*, Xinjiang Seismological Bureau, Eds. (Xinjiang Press, Urumqi, China, 1988), pp. 66–71.
18. G. Peltzer, F. Crampe, G. King, *Science* **286**, 272 (1999).
19. W. S. F. Kidd, P. Molnar, *Philos. Trans. R. Soc. London Ser. A* **327**, 337 (1988).
20. G. Peltzer, F. Saucier, *J. Geophys. Res.* **101**, 27943 (1996).
21. Z. Shen *et al.*, *J. Geophys. Res.* **106**, 30607 (2001).
22. Q. Wang *et al.*, *Science* **294**, 574 (2001).
23. K. M. Larson *et al.*, *J. Geophys. Res.* **104**, 1077 (1999).

24. We thank J. Du, T. Matsuda, S. Wu, K. Kano, and Z. Yang for constructive discussions and Z. Wang and E. W. Woolery for critical reading of the manuscript that greatly improved this paper. Supported by the Laboratory of Geomechanics, Institute of Geomechanics, Chinese Academy of Geological Sciences; the Commemoration Part of the Nojima Earthquake Fault, Hokudan-cho, Hyogo Prefecture, Japan; and the Science Project of the Ministry of Education, Culture, Sports, Science and Technology of Japan.

Supporting Online Material

www.sciencemag.org/cgi/content/full/296/5575/2015/DC1

Figs. S1 to S3

Tables S1 and S2

14 February 2002; accepted 8 May 2002